



## Analytical Methods

# Electrochemical behavior and voltammetric determination of vanillin based on an acetylene black paste electrode modified with graphene–polyvinylpyrrolidone composite film



Peihong Deng<sup>a,\*</sup>, Zhifeng Xu<sup>a</sup>, Rongying Zeng<sup>a,b</sup>, Chunxia Ding<sup>c</sup>

<sup>a</sup> Department of Chemistry and Material Science, Hengyang Normal University, Hengyang 421008, PR China

<sup>b</sup> College of Resource and Environment, Hunan Agricultural University, Changsha 410128, PR China

<sup>c</sup> College of Science, Hunan Agricultural University, Changsha 410128, PR China

## ARTICLE INFO

## Article history:

Received 7 October 2014

Received in revised form 8 February 2015

Accepted 9 February 2015

Available online 14 February 2015

## Keywords:

Graphene–polyvinylpyrrolidone composite film

Electrochemical sensor

Vanillin

Electrochemical behavior

Voltammetric determination

## ABSTRACT

The graphene–polyvinylpyrrolidone composite film modified acetylene black paste electrode (GR–PVP/ABPE) was fabricated and used to determine vanillin. In 0.1 M H<sub>3</sub>PO<sub>4</sub> solution, the oxidation peak current of vanillin increased significantly at GR–PVP/ABPE compared with bare ABPE, PVP/ABPE and GR/ABPE. The oxidation mechanism was discussed. The experimental conditions that exert influence on the voltammetric determination of vanillin, such as supporting electrolytes, pH values, accumulation potential and accumulation time, were optimized. Besides, the interference, repeatability, reproducibility and stability measurements were also evaluated. Under the optimal experimental conditions, the oxidation peak current was proportional to vanillin concentration in the range of 0.02–2.0 μM, 2.0–40 μM and 40–100 μM. The detection limit was 10 nM. This sensor was used successfully for vanillin determination in various food samples.

© 2015 Elsevier Ltd. All rights reserved.

## 1. Introduction

Vanillin (4-hydroxy-3-methoxybenzaldehyde) is the major component of natural vanilla. The desirable flavor and aroma properties of vanillin have led to its widespread application in confectionery, beverage, pharmaceutical, food and perfumery industries. Vanillin is reported to have beneficial health effects such as inhibition of the oxidation of human low density lipoproteins leading to lower rates of cardiac disease mortality (Teissedre & Waterhouse, 2000) and an antisickling effect in sickle cell anaemia sufferers (Farthing et al., 1999). The source of vanilla is the bean, or pod, of a tropical *Vanilla* orchid. Although more than 12,000 tons of vanilla is produced each year, less than 1% of this is natural vanillin from *Vanilla*, the remainder is synthesized much more cheaply via chemical or biochemical processes (Walton, Mayer, & Narbad, 2003). Although synthetic vanillin is cheaper and widely produced, extensive evidence indicates that excessive ingestion of vanillin can cause headaches, nausea and vomiting, and it can also affect the function of the liver and kidney. Therefore, simple, sensitive and low-cost determination of vanillin is of great significance to people's health.

Nowadays, many analytical methods have been proposed for vanillin accurate determination in various food samples or vanilla extracts, such as high performance liquid chromatography (Farthing et al., 1999; Waliszewski, Pardio, & Ovando, 2006) gas chromatography (Pérez-Silva et al., 2006), capillary electrophoresis (Ohashi, Omae, Hashida, Sowa, & Imai, 2007), UV–vis spectrophotometry (Longares-Patrón & Cañizares-Macías, 2006) and chemiluminescence (Timotheou-Potamia & Calokerinos, 2007). With the advantages of cheap instrumentation, small sample volume and rapid analysis, the electrochemical sensor is an ideal technique for the determination of vanillin because the molecule is electrooxidisable. However, a major obstacle encountered in the detection of vanillin at bare electrode is the relatively high overpotential together with poor reproducibility resulted from a fouling effect, which causes rather poor selectivity and sensitivity (Hardcastle, Paterson, & Compton, 2001). An effective way to overcome these barriers is electrode modification. Some chemically modified electrodes have been reported (Bettazzi, Palchetti, Sisalli, & Mascini, 2006; Kong, Shen, Yu, Wang, & Chen, 2010; Luque, Luque-Pérez, Ríos, & Valcárcel, 2000; Peng, Hou, & Hu, 2012; Shang, Zhao, & Zeng, 2014; Yardım, Gülcan, & SŞentürk, 2013; Zheng, Hu, Gan, Dang, & Hu, 2010). However, the performance of some electrodes was still not enough good. Thus it is important to develop new modified electrodes for vanillin detection.

\* Corresponding author. Tel.: +86 13908447066.

E-mail address: [dph1975@163.com](mailto:dph1975@163.com) (P. Deng).

Graphene (GR) has attracted enormous attention among researchers for its properties such as high thermal conductivity, high electrical conductivity and electron transfer rate (Li & Kaner, 2008). Thus GR was chosen as the electrode material in this research. However, the practical applications of GR are challenged by its irreversible agglomeration both in the drying state and in common solvents, which significantly reduces its effectiveness (Niyogi et al., 2006; Pasricha, Gupta, & Srivastava, 2009). In the present work, polyvinylpyrrolidone (PVP) was dissolved in water as the solvent to disperse GR, which can make GR dispersed more evenly, and can be better fixed on the electrode surface.

Recently, acetylene black (AB) with novel properties such as large specific surface area, strong adsorptive ability, excellent electric conductivity was developed and has been widely used in electrochemical sensors. As far as we are aware no work on the determination of vanillin by combination of the excellent properties of GR and AB has been reported previously, a novel electrochemical sensor was developed for vanillin determination using GR–PVP composite film modified acetylene black paste electrode (denoted as GR–PVP/ABPE). The electrochemical behaviors of vanillin were investigated on GR–PVP/ABPE carefully with the electrochemical parameters calculated. Finally, the fabricated sensor was applied to determine trace amounts of vanillin in food samples and the results were consistent with those obtained by HPLC. This method offers several advantages over other techniques, including being of low environmental impact, efficient, inexpensive and rapid.

## 2. Experimental

### 2.1. Chemicals and solutions

Graphite powder, hydrazine hydrate solution (80 wt%), polyvinylpyrrolidone and vanillin were purchased from Sinopharm Chemical Reagent Co., Ltd., Shanghai, China. Acetylene black (AB, purity > 99.99%) was supplied by STREM Chemicals, USA. A standard stock solution of  $1.0 \times 10^{-3}$  M vanillin was prepared by dissolving vanillin in ethanol, which was preserved at 4 °C and protected from daylight when not in use. Working solutions of lower concentrations were prepared by appropriate dilution of the stock solution with 5% (v/v) ethanol aqueous solution. 0.1 M  $\text{H}_3\text{PO}_4$  solution was used as the supporting electrolyte. All other chemicals were of analytical reagent grade and used without further purification. All solutions were prepared with doubly distilled water.

### 2.2. Apparatus

Cyclic voltammetry was performed on a CHI 660E electrochemical workstation (Chenhua Instrument Co., Ltd., Shanghai, China) controlled by a microcomputer with CHI660 software. Second-order derivative linear sweep voltammograms were measured on a model JP-303E polarographic analyzer (Chengdu Instrument Factory, Chengdu, China). A conventional three-electrode system was adopted. The working electrode was a GR–PVP/ABPE (diameter: 1 mm), the auxiliary and reference electrodes were a platinum wire and a saturated calomel electrode (SCE), respectively. JEOL JSM-6610LV scanning electron microscope (Jeol/Ntc., Japan) was used for the characterization of GR–PVP composite. The pH measurements were carried out on a pHs-3c exact digital pH meter (Shanghai Leichi Instrument Factory, Shanghai, China), which was calibrated with standard pH buffer solutions. High-performance liquid chromatography (HPLC) was performed on Waters model 510 system (Waters Ltd., USA) comprising a Kromasil 100-5C18 (250 mm  $\times$  4.6 mm) column equipped with a Waters 2487

dual  $\lambda$  absorbance UV/Vis detector using a mobile phase consisting of aqueous acetic acid (1%, v/v)–acetonitrile (85:15, v/v) at a flow rate of 0.6 mL min<sup>-1</sup>.

### 2.3. Preparation of GR–PVP dispersion

Graphite oxide were synthesized from natural graphite powder according to our previous reports (Deng, Xu, & Feng, 2014; Deng, Xu, & Kuang, 2013) and dispersed in water to form a 0.5 mg mL<sup>-1</sup> graphene oxide (GO) dispersion by ultrasonication for 2 h. 10.0 mg of PVP was added into the 20 mL GO dispersion in a flask. After magnetic stirring for 10 min, the resulting dispersion was further treated with 20  $\mu$ L of 80 wt% hydrazine hydrate solution and 80  $\mu$ L of 25 wt% ammonia solution and allowed to react for 1 h at 95 °C. Finally, the color of mixture solution changed from light yellow to black at the end of the reaction, indicating the reduction of GO. The black GR–PVP suspension was stable for at least 2 months at room temperature. As a control, the pure GR suspension was prepared in the same way mentioned above but without the addition of PVP.

### 2.4. Fabrication of modified electrodes

The acetylene black paste electrode (ABPE) was prepared by thoroughly mixing 1.20 g acetylene black powder with 0.30 g solid paraffin in a mortar, and then the mixture was heated at 80 °C until the solid paraffin melted. The resultant paste was tightly pressed into the end cavity (1 mm in diameter) of the electrode body immediately, and the surface was polished with a piece of smooth paper until it had a shiny appearance. The electrode was subjected to cyclic potential sweeps between 0.2 and 1.2 V in 0.5 M  $\text{H}_2\text{SO}_4$  solution until a stable cyclic voltammogram was obtained. A volume of 2  $\mu$ L of the resulting GR–PVP dispersion was casted onto the surface of ABPE and dried at room temperature. For comparison, the PVP/ABPE and GR/ABPE were prepared by casting 2  $\mu$ L of 0.5 mg mL<sup>-1</sup> PVP and 2  $\mu$ L of 0.5 mg mL<sup>-1</sup> GR onto the ABPE surface respectively. In order to show the unique properties of AB, the ordinary carbon paste electrode made of graphite powder (CPE) was also prepared.

### 2.5. Pretreatment of the commercial food samples

Various kinds of food products such as biscuit, chocolate, candy, cake, soy milk powder, icecream, orange flavored soft drink and colo were purchased from a local supermarket. The sample solutions were prepared by the following procedure. Solid samples taken from five packages of the same brand were carefully ground to a fine powder and mixed adequately in the mortar. An accurately weighed portion of powder (about 1.0 g) was taken and dispersed in 10 mL ethanol. The mixture was sonicated for 1 h with a supersonic cleaner. After centrifugating (4000 rpm) for 10 min, 0.50 mL of the clear supernatant was diluted to 10 mL with 0.10 M  $\text{H}_3\text{PO}_4$  for voltammetric determination. The liquid samples were transferred into beaker and degassed in an ultrasonic bath. Then 1.0 mL of the samples was pipetted into the voltammetric cell, and diluted to 10 mL with 0.10 M  $\text{H}_3\text{PO}_4$  solution for voltammetric determination.

### 2.6. Experimental procedure

For voltammetric measurements, the three-electrode system was immersed in a 10-mL electrochemical cell containing an appropriate concentration of vanillin and 0.1 M  $\text{H}_3\text{PO}_4$  solution. The solution was stirred at 500 rpm at a chosen accumulation potential throughout the selected accumulation period. Following the pre-concentration period, the stirring was stopped, and after

a 5 s had elapsed, cyclic voltammograms or second-order derivative linear sweep voltammograms were recorded at a scan rate of  $0.1 \text{ V s}^{-1}$ . The potential scan ranges were 0.2–1.2 V for cyclic voltammograms and 0.7–1.2 V for the second-order derivative linear sweep voltammograms. The same procedure was carried out in the sample analysis and all electrochemical experiments were performed at room temperature.

### 3. Results and discussion

#### 3.1. Morphological analysis

In this work, GO was reduced to GR by hydrazine hydrate in the presence of PVP, and the obtained GR–PVP suspension showed excellent dispersibility and long-term stability. The morphology of the GR–PVP composite was observed by scanning electron microscopy (SEM). As shown in Fig. 1(A), the SEM image showed that graphene consists of aggregated, crumpled, thin sheets in a random manner closely associated with each other. As reported previously, corrugation and scrolling were intrinsic to graphene

nanosheets (Meyer et al., 2007). This wrinkled nature of graphene was highly beneficial in maintaining a high surface area on the electrode. The inset of Fig. 1(A) shows the photographs of pure GR and GR–PVP aqueous dispersion after 2 months storage. The results demonstrated that the pure GR has a distinctly poor dispersion and stability in water, which generated a little precipitate after several days, and completely settled down upon 2 months of standing (inset (a)), while GR–PVP composite can form very stable and homogeneous dispersion even for months of storage (inset (b)). Since the dispersion of nanomaterials in solution is crucial to their further application (Li, Müller, Gilje, Kaner, & Wallace, 2008), GR–PVP is considered practicable and advisable for further application.

#### 3.2. Characteristic of the modified electrodes by cyclic voltammetry

Cyclic voltammetry can provide interface information of the electrode surface during the modification process. The cyclic voltammetric behaviors of  $1.0 \text{ mM K}_3[\text{Fe}(\text{CN})_6]$  containing  $0.1 \text{ M KCl}$  at different electrodes were studied at a potential scan rate of  $0.1 \text{ V s}^{-1}$ . As shown in Fig. 1(B), on the CPE (curve a), the peak-to-peak potential separation ( $\Delta E_p$ ) was  $0.120 \text{ V}$  with small redox peak currents, corresponding to a quasi-reversible electron transfer process. On the ABPE (curve b), a pair of well-defined redox peaks appeared while the redox peak current increased and the  $\Delta E_p$  obviously decreased to  $0.108 \text{ V}$ , which indicated the presence of the high conductivity of AB on the electrode surface. After casting GR on the ABPE (curve c), the redox peaks clearly increased with  $\Delta E_p$  value as  $0.096 \text{ V}$ , which was due to the large surface area and excellent electrical conductivity of GR present on the electrode surface. When GR–PVP was fixed on the ABPE surface (curve d), the redox peak currents further increased with  $\Delta E_p$  value of  $0.112 \text{ V}$ . As indicated above, PVP can be used as an effective disperser to disperse GR nanosheets in aqueous solution. The prevention of aggregation is of particular importance for GR because most of the unique properties are only associated with individual sheet. According to the Randles–Sevcik equation (Bard & Faulkner, 2001):  $i_{pc} = (2.69 \times 10^5) n^{3/2} D^{1/2} \nu^{1/2} A C$ , where  $i_{pc}$  is the reduction peak current (A),  $n$  is the electron transfer number,  $A$  is the electroactive surface area ( $\text{cm}^2$ ),  $D$  is the diffusion coefficient of  $\text{K}_3[\text{Fe}(\text{CN})_6]$  in the solution ( $7.6 \times 10^{-6} \text{ cm}^2 \text{ s}^{-1}$ ) (Gooding, Praig, & Hall, 1998),  $C$  is the concentration of  $\text{K}_3[\text{Fe}(\text{CN})_6]$  ( $\text{mol cm}^{-3}$ ) and  $\nu$  is the scan rate ( $\text{V s}^{-1}$ ). By exploring the redox peak current with scan rate, the average electroactive areas of CPE, ABPE, GR/ABPE and GR–PVP/ABPE were calculated as  $0.00465 \text{ cm}^2$ ,  $0.01671 \text{ cm}^2$ ,  $0.02553 \text{ cm}^2$  and  $0.0309 \text{ cm}^2$ , respectively. The results further indicated the presence of GR–PVP composite film greatly improved the effective area of the electrode surface, which led to the great enhancement of electrochemical response on the modified electrode.

#### 3.3. Voltammetric behavior of vanillin at the GR–PVP/ABPE

The electrochemical behavior of  $50 \mu\text{M}$  vanillin on the GR–PVP/ABPE was studied first by cyclic voltammetry, and the results are presented in Fig. 2(A). As shown in Fig. 2(A), a sensitive and well-defined oxidation peak ( $P_1$ ) appeared at  $0.964 \text{ V}$  during the first anodic sweep from  $0.2 \text{ V}$  to  $1.2 \text{ V}$ . There is no doubt that the peak should be attributed to the oxidation of vanillin. On the reverse scan, a reduction peak ( $P_2$ ) appeared at  $0.602 \text{ V}$ . During the second anodic sweep, in addition to  $P_1$ , another oxidation peak ( $P_3$ ), which was at  $0.697 \text{ V}$  and formed a redox couple with peak  $P_2$ , was observed. At the same time, the oxidation peak current of  $P_1$  in the second cyclic sweep decreased remarkably compared with that of the first cyclic sweep. It is very interesting that the quasi-reversible redox couple ( $P_2/P_3$ ) increased at the expense of the

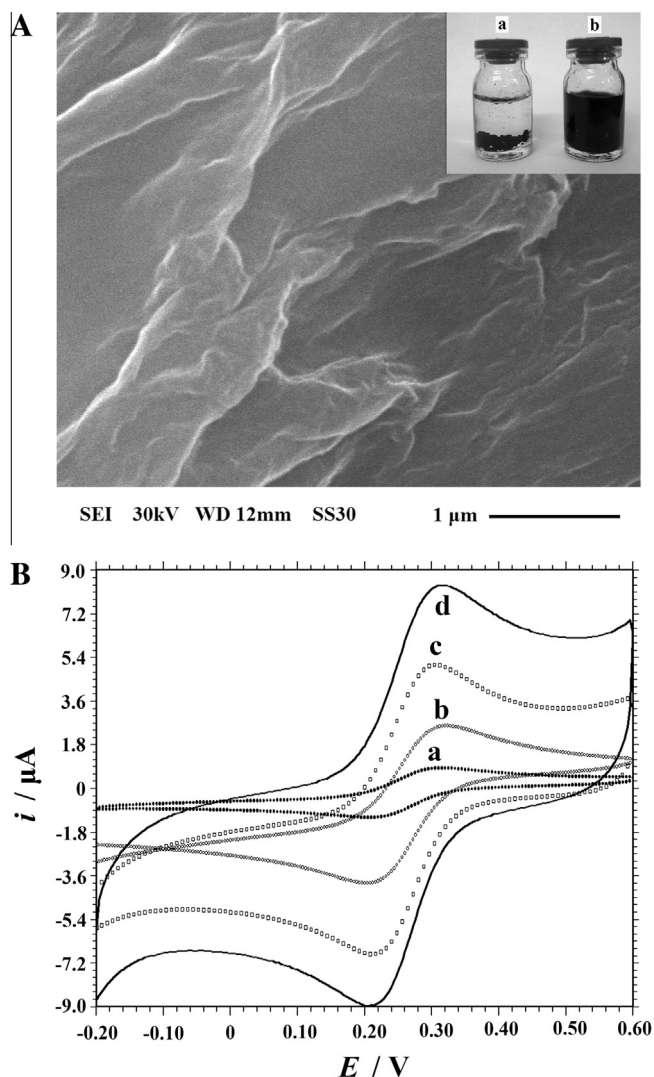


**Fig. 1.** (A) SEM image of GR–PVP/ABPE. Accelerating voltage: 30 kV; magnification times: 20,000. Inset: photographs of pure GR (a) and PVP–GR (b) aqueous suspensions. (B) Cyclic voltammograms of  $1.0 \text{ mM}$  potassium ferricyanide in  $0.1 \text{ M KCl}$  solution recorded at different electrodes: (a) CPE, (b) ABPE, (c) GR/ABPE and (d) GR–PVP/ABPE. Scan rate:  $0.1 \text{ V s}^{-1}$ .



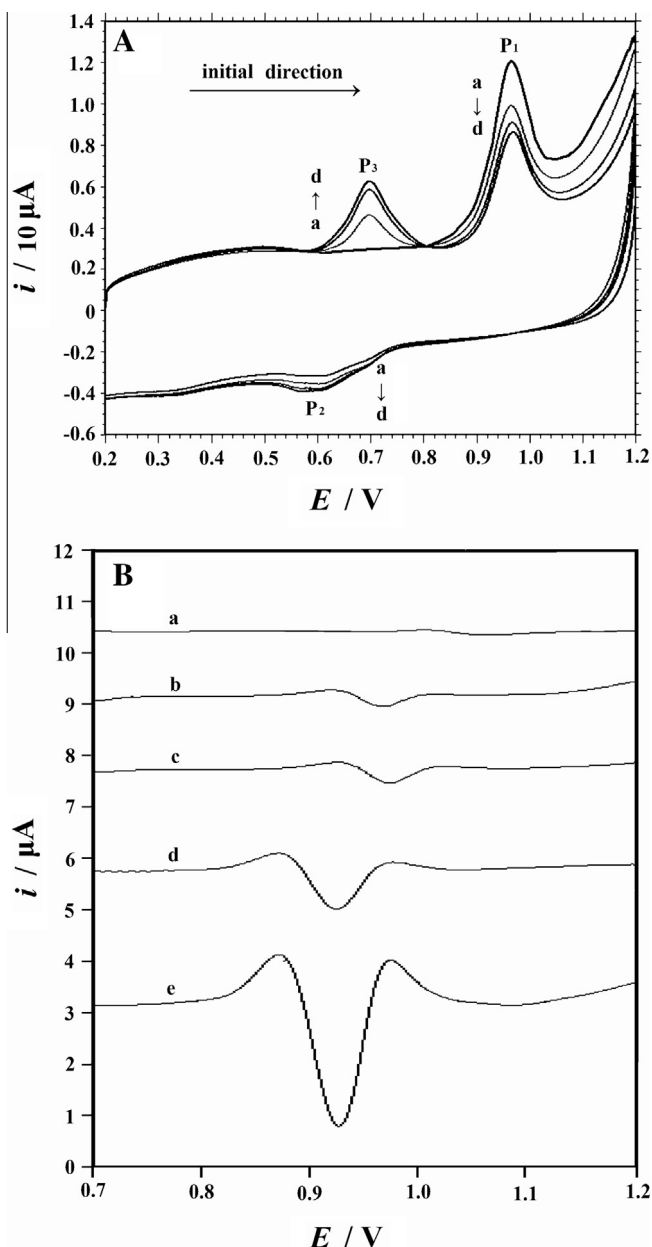


**Fig. 2.** (A) Cyclic voltammograms of 50  $\mu M$  vanillin in 0.1 M  $H_3PO_4$  on GR-PVP/ABPE by continuous sweep cycles. (a)–(d) 1st–4th. (B) Second-order derivative linear scan voltammograms of 50  $\mu M$  vanillin in 0.1 M  $H_3PO_4$  obtained at (a) CPE, (b) ABPE, (c) PVP/ABPE, (d) GR/ABPE and (e) GR-PVP/ABPE. Accumulation potential: 0.0 V, accumulation time: 60 s, scan rate: 0.1  $V s^{-1}$ .

irreversible peak ( $P_1$ ), indicating that the product of vanillin by irreversible oxidation remained on or close to the modified electrode surface and was reduced on the cathodic sweep. If the initial anodic sweep is reversed before 0.8 V under the same conditions, i.e. before peak  $P_1$ , the redox couple  $P_2/P_3$  will disappear. These results suggest that the development of  $P_1$  peak is responsible for the formation of the redox couple  $P_2/P_3$ . From Fig. 2(A) it is very clear that the oxidation peak  $P_1$  is much more sensitive than the redox couple  $P_2/P_3$ . Therefore, the oxidation peak  $P_1$  was selected as the response signal for the determination of vanillin in this work.

Second-order derivative linear sweep voltammetry is a widely used analytical technique for the enhancement of sensitivity and specificity in quantitative analysis (Liu, Li, & Mao, 2003). Fig. 2(B)

shows the second-order derivative linear sweep voltammetric responses of 50  $\mu M$  vanillin at the bare CPE (a), ABPE (b), PVP/ABPE (c), GR/ABPE (d) and GR-PVP/ABPE (e). As shown in Fig. 2(B), a relatively broad and weak oxidation peak (1046 mV, 0.095  $\mu A$ ) was observed on the surface of the bare CPE which reveals that the unmodified electrode process is not spontaneous because of high activation overpotential. While on the ABPE, vanillin yielded an anodic peak at 976 mV and the peak current increased to 0.2663  $\mu A$ . These phenomena suggest that the oxidation of vanillin is more favorable at the ABPE, which is undoubtedly attributed to the unique characteristics of AB such as excellent electric conductivity, high surface area and strong adsorptive abilities. When PVP was modified on ABPE surface, the peak current increased slightly (0.3500  $\mu A$ ), which might arise from the hydrogen bonding interactions between imide moieties of PVP and hydroxyl group in vanillin. When the GR/ABPE was used, the peak shifted negatively to 924 mV, and the peak current increased to 1.025  $\mu A$ . The remarkable enhancement of the peak current and the lowered overpotential are clear evidence of the enhancement effects of GR on vanillin oxidation. Compared with the GR/ABPE, the peak current of vanillin obtained at GR-PVP/ABPE was further increased (3.357  $\mu A$ ), which was approximate 35 times as much as that of the bare CPE, and the peak shape was sharp. This phenomenon may be attributed to the attractive characteristics of GR, PVP and AB. On the one hand, because vanillin was one kind of aromatic compounds, it could be adsorbed by GR and PVP through  $\pi$ - $\pi$  stacking and hydrogen bonding. On the other hand, due to the good dispersion of GR in the presence of PVP and excellent conductivity of AB, the electron transfer rate of vanillin was greatly accelerated.

The effect of solution pH on the electrochemical response of the sensor toward the determination of vanillin was studied. The variations of peak current as well as the oxidation peak potential with respect to the change of the electrolyte in the pH range from 1.65 to 5.07 are shown in Fig. S1 (presented in Electronic Supplementary material, ESM). It can be seen in Fig. S1(B) the oxidation peak current decreased gradually with increasing the pH, indicating that protons have taken part in the electrode reaction processes. The relationship between the oxidation peak potential ( $E_p$ ) and pH is also shown in Fig. S1(C). It is found that the value of the oxidation peak potential ( $E_p$ ) shifted to more negative potential with the increase of pH from 1.65 to 5.07, and that it obeys the following equation:  $E_p (V) = -0.0534 \text{ pH} + 1.0276$  ( $R = 0.9994$ ). A shift of typically 53.4 mV per pH unit is approximately close to the theoretical value of 57.6 mV per pH unit (Bard & Faulkner, 2001), indicating that the electron transfer is accompanied by an equal number of protons in electrode reaction.

Cyclic voltammograms of the fabricated GR-PVP/ABPE at different scan rates were also recorded (Fig. S2). It is clear that the peak currents increase with the rising of scan rate from 20 to 200  $mV s^{-1}$ , while the peak potentials shift positively. It is observed that the peak currents increase linearly with the square root of scan rate, and the linear regression equation can be expressed as  $i (\mu A) = 0.5645 v^{1/2} (mV s^{-1}) - 1.2957$  ( $R = 0.9972$ ), indicating that the oxidation of vanillin is under diffusion control. The diffusion or adsorption controlled behavior was also confirmed by plotting  $\log i$  vs.  $\log v$  corresponding to the equation:  $\log i (\mu A) = 0.6731 \log v (mV s^{-1}) - 0.7177$  ( $R = 0.9995$ ) (Fig. S2(B)). The obtained slope of 0.6731 is close to 0.5 which confirms largely diffusion controlled nature of the electrode process. Similarly, a linear relationship between  $E_p$  and Napierian logarithm of  $v$  ( $\ln v$ ) is also observed in the range of 20–200  $mV s^{-1}$  (Fig. S2(C)). The equation can be expressed as  $E_p (V) = 0.021 \ln v + 0.8958$  ( $R = 0.9991$ ). According to Laviron's theory (Laviron, 1974), the slope of the line is equal to  $RT/(\alpha nF)$ . Therefore,  $\alpha n$  is calculated to be 1.2. Generally, for a totally irreversible electrode process,  $\alpha$  is assumed to be 0.5, so the electron transfer number ( $n$ ) involved

in the oxidation process of vanillin is around 2. Considering that the number of electrons and protons involved in the oxidation process of vanillin is equal as demonstrated in the pH-dependent electrochemical response, the electrooxidation of vanillin ( $P_1$ ) at GR-PVP/ABPE is a two-electron and two-proton process.

In order to ascertain the number of electrons involved in the redox process ( $P_2/P_3$ ) at the GR-PVP/ABPE, we determined the value of  $n$  from cyclic voltammograms (Fig. 2(A)) by using the following equation (Galus, 1976):

$$n = 0.0565 / (E_p - E_{p/2}) \quad (1)$$

$n$  was calculated to be 2.017 at GR-PVP/ABPE, which suggests that the number of the electrons corresponding to the redox process ( $P_2/P_3$ ) is two. Based on the results obtained, we believe the electron transfer mechanism can be illustrated as Scheme 1. Similar behavior of vanillin has also been observed in previous reports (Gan, Shi, Deng, Sun, & Wang, 2014; Huang, Hou, Jia, Pan, & Du, 2014).

The electrooxidation of vanillin at the GR-PVP/ABPE was also studied by chronocoulometry. The corresponding chronocoulometric curves were shown in Fig. 3. According to Anson's equation (Anson, 1964):

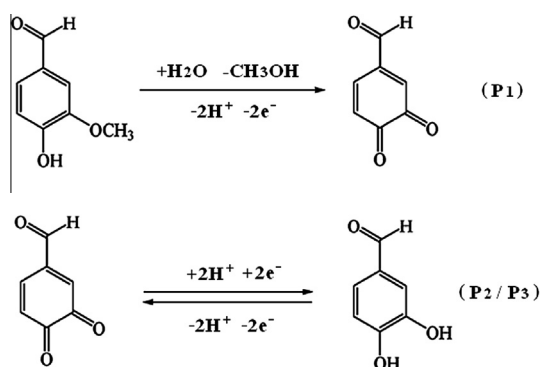
$$Q = 2nFAcD^{1/2}\pi^{-1/2}t^{1/2} + Q_{dl} + Q_{ads} \quad (2)$$

where  $n$  is the number of electron transferred,  $F$  ( $C \text{ mol}^{-1}$ ) is the Faraday constant,  $A$  ( $\text{cm}^2$ ) is the surface area of the working electrode,  $c$  ( $\text{mol cm}^{-3}$ ) is the concentration of vanillin,  $D$  ( $\text{cm}^2 \text{s}^{-1}$ ) is the diffusion coefficient,  $Q_{dl}$  (C) is the double layer charge which could be eliminated by background subtraction,  $Q_{ads}$  (C) is the adsorption charge, other symbols have their usual significances. The diffusion coefficient  $D$  and Faradic charge  $Q_{ads}$  of vanillin at GR-PVP/ABPE can be determined based on Eq. (2). As shown in Fig. 3(B), after point-by-point background subtraction, the plot of charge ( $Q$ ) against the square root of time ( $t^{1/2}$ ) showed a linear relationship with slope of  $1.330 \times 10^{-6} \text{ C s}^{-1/2}$  and  $Q_{ads}$  of  $4.906 \times 10^{-7} \text{ C}$ . As  $n = 2$ ,  $c = 1.0 \times 10^{-7} \text{ mol cm}^{-3}$ , and  $A$  was  $0.0309 \text{ cm}^2$  described in Section 3.2, it was calculated that  $D = 3.9 \times 10^{-6} \text{ cm}^2 \text{s}^{-1}$  at GR-PVP/ABPE.

The standard heterogeneous rate constant ( $k_s$ ) for totally irreversible oxidation of vanillin at the GR-PVP/ABPE was calculated based on Eq. (3) (Velasco, 1997):

$$k_s = 2.415 \exp(-0.02F/RT)D^{1/2}(E_p - E_{p/2})^{-1/2}v^{1/2} \quad (3)$$

where  $E_p$  and  $E_{p/2}$  represent the peak potential and the potential at which  $i = i_p/2$  in linear sweep voltammetry (LSV), respectively. Other symbols have their usual meanings. In our experiment,  $E_p - E_{p/2} = 44 \text{ mV}$ ,  $D = 3.9 \times 10^{-6} \text{ cm}^2 \text{s}^{-1}$ ,  $v = 100 \text{ mV s}^{-1}$ , and  $T = 298 \text{ K}$ . The  $k_s$  value was calculated to be  $3.30 \times 10^{-3} \text{ cm s}^{-1}$ .



Scheme 1. The reaction mechanism of vanillin on the GR-PVP/ABPE.

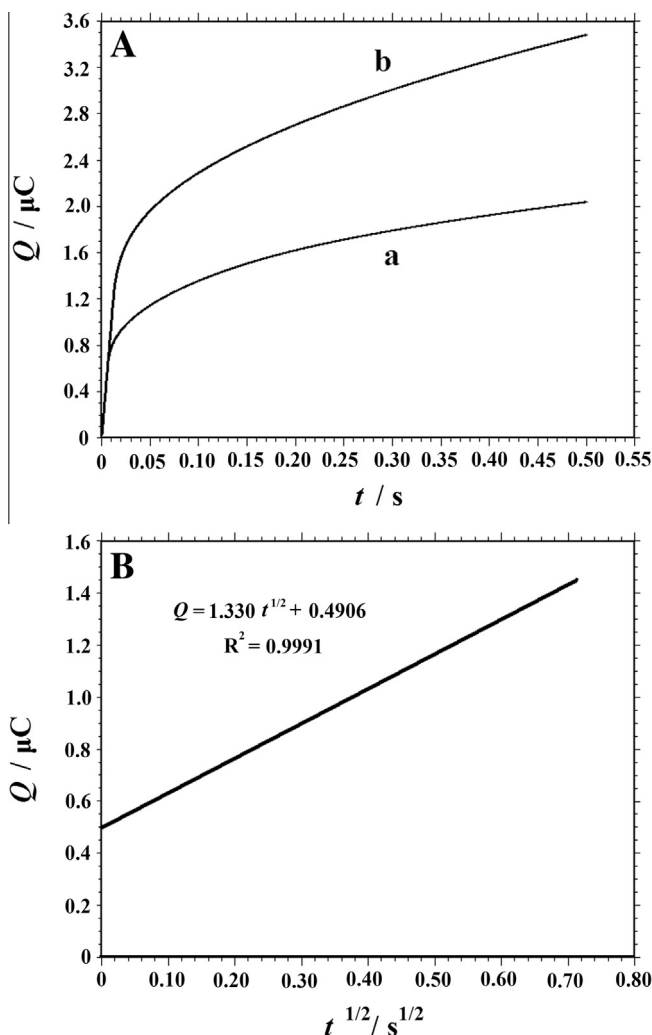


Fig. 3. (A) Chronocoulometric curves for GR-PVP/ABPE in 0.1 M  $\text{H}_3\text{PO}_4$  in absence of (a) and in presence of (b) 0.1 mM vanillin. (B) Plot of  $Q - t^{1/2}$  curve for GR-PVP/ABPE in presence of 0.1 mM vanillin (background subtracted).

### 3.4. Optimization of experimental parameters

#### 3.4.1. Choice of supporting electrolyte

Second-order derivative linear sweep voltammetry was used to study the effect of type of supporting electrolyte on the oxidation peak current of  $50 \mu\text{M}$  vanillin. Different supporting electrolytes were tested, including phosphate buffer, Britton–Robinson buffer,  $\text{HAc-NH}_4\text{Ac}$  buffer,  $\text{HAc-NaAc}$  buffer,  $(\text{CH}_2)_6\text{N}_4\text{-HCl}$  buffer and some different acids and alkalies such as  $\text{HCl}$ ,  $\text{H}_2\text{SO}_4$ ,  $\text{HNO}_3$ ,  $\text{H}_3\text{PO}_4$ ,  $\text{HClO}_4$  and  $\text{NaOH}$  (each  $0.1 \text{ M}$ ). It was found that when  $0.1 \text{ M H}_3\text{PO}_4$  solution was used, the oxidation peak current was much larger and the baseline was smooth and steady, which resulted in a high sensitivity. For further study,  $0.1 \text{ M H}_3\text{PO}_4$  solution was chosen as the supporting electrolyte.

#### 3.4.2. Effect of accumulation conditions

In order to evaluate the influence of accumulation potential on the determination of vanillin, the oxidation peak currents of  $10 \mu\text{M}$  vanillin after  $60 \text{ s}$  accumulation under different accumulation potentials were measured. The peak currents almost keep unchanged when the accumulation potential shifted from  $-0.3$  to  $0.6 \text{ V}$ , revealing that the accumulation potential has no influence on the oxidation peak current of vanillin at the GR-PVP/ABPE. Thus, the accumulation step was performed under  $0.0 \text{ V}$ . The

dependence of the oxidation peak current on the accumulation time was also investigated. As shown in Fig. S3, the peak current increased gradually with accumulation time up to 60 s at a fixed accumulation potential of 0.0 V. Afterwards, the peak current increased much slightly as further increasing accumulation time. This phenomenon could be attributed to the saturated adsorption of vanillin at the electrode surface. Considering both sensitivity and work efficiency, the optimal accumulation time of 60 s was employed in the further experiments.

### 3.5. Repeatability, reproducibility and stability of GR-PVP/ABPE

Repeatability, reproducibility and stability are three important characteristics for the modified electrode. The most attractive feature with the use of GR-PVP/ABPE for determination of vanillin is the easy renewal of surface for the next use. When scanning linearly from 0.7 V to 1.2 V, the used electrode surface can be renewed by two successive voltammetric sweeps within the same potential range in 0.1 M  $\text{H}_3\text{PO}_4$ , and a relative standard deviation (RSD) of ten measurements for 50  $\mu\text{M}$  vanillin using the same electrode was 2.83%, which indicated that the adsorption of oxidative product of vanillin at the electrode surface is weak and can be desorbed from the surface easily in blank acidic media. The fabrication reproducibility was also estimated. Seven electrodes were made by the same procedure independently and the RSD value for the determination of 50  $\mu\text{M}$  vanillin was calculated as 5.37%, which indicated the reliability of the fabrication procedure. Additionally, the stability of GR-PVP/ABPE was also investigated. When the modified electrode was stored in air at room temperature for 10 days, the peak current retained 93% of its original response.

### 3.6. Interference studies

In order to evaluate the selectivity of the prepared sensor, the influence of selected potential interfering compounds such as inorganic ions and organic compounds, was examined. It was observed that  $\text{K}^+$ ,  $\text{Na}^+$ ,  $\text{Ca}^{2+}$ ,  $\text{Mg}^{2+}$ ,  $\text{Pb}^{2+}$ ,  $\text{Cd}^{2+}$ ,  $\text{Al}^{3+}$ ,  $\text{Cu}^{2+}$ ,  $\text{Zn}^{2+}$ ,  $\text{Cl}^-$ ,  $\text{NO}_3^-$ ,  $\text{SO}_4^{2-}$ , oxalic acid, citric acid, glucose, lactic acid, tartaric acid, benzoic acid, fructose, sucrose and cholesterol showed no obvious interference to the determination of 10  $\mu\text{M}$  vanillin even when present 100 times in excess, with deviations below 5%. Interference due to some related phenolic compounds which may be present together with vanillin in different types of samples (food and perfumery items) was tested. Experimental results showed when 10-fold concentration of guaiacol, chlorogenic acid, caffeic acid, p-hydroxybenzoic acid, 5-fold concentration of p-hydroxybenzaldehyde, 2-fold concentration of ferulic acid, syringic aldehyde and sinapic acid was present, the change of peak current of 10  $\mu\text{M}$  vanillin was less than <5%. The interferences from some electroactive biomolecules were also examined. Fig. S4 showed the second-order derivative linear sweep voltammograms of 10  $\mu\text{M}$  vanillin at PVP-GR/ABPE when coexisting with 1.0 mM ascorbic acid (AA) and 0.1 mM uric acid (UA). The results indicated that the oxidation of vanillin at GR-PVP/ABPE occurred at a very positive potential ( $E_p = 0.926$  V), which was much higher than the oxidation potentials of AA ( $E_p = 0.300$  V) and UA ( $E_p = 0.712$  V). Thus, the interferences of AA and UA were neglected even when an interferent-to-analyte ratio of 100:1 was used. These results confirmed that the GR-PVP/ABPE had a good selectivity for vanillin determination.

### 3.7. Calibration curve

In order to obtain an analytical curve for the fabricated sensor, the quantitative analysis of vanillin concentration using GR-PVP/ABPE was performed with second-order derivative linear sweep

voltammetry under the optimized experimental conditions and the results are shown in Fig. 4. It can be seen that an increase in vanillin concentration is accompanied by an increase in oxidation current. The calibration curve shows three linear regions (0.02–2.0  $\mu\text{M}$ , 2.0–40  $\mu\text{M}$  and 40–100  $\mu\text{M}$ ) in this relationship. The linear regression equations for these ranges were  $i$  ( $\mu\text{A}$ ) =  $(0.1714 \pm 0.0018)c$  ( $\mu\text{M}$ ) –  $(0.0014 \pm 0.0001)$ ,  $i$  ( $\mu\text{A}$ ) =  $(0.0805 \pm 0.0016)c$  ( $\mu\text{M}$ ) +  $(0.2662 \pm 0.0153)$  and  $i$  ( $\mu\text{A}$ ) =  $(0.0269 \pm 0.0007)c$  ( $\mu\text{M}$ ) +  $(2.3851 \pm 0.0268)$  with correlation coefficient  $R = 0.9985$ , 0.9959 and 0.9985, respectively (intercept and slope in the regression equations were presented as average  $\pm$  SD,  $n = 4$ ). The detection limit ( $S/N = 3$ ) was estimated to be 10 nM. The three concentration ranges with different slopes are probably caused by changing contributions of adsorptive and diffusion current components that is often observed for wide concentration range (3–4 orders).

In order to make a realistic comparison with previous procedures, comparative analytical figures of merit for different electrodes for the determination of vanillin were obtained (Table 1). As it is obvious, the performance of the GR-PVP/ABPE is superior

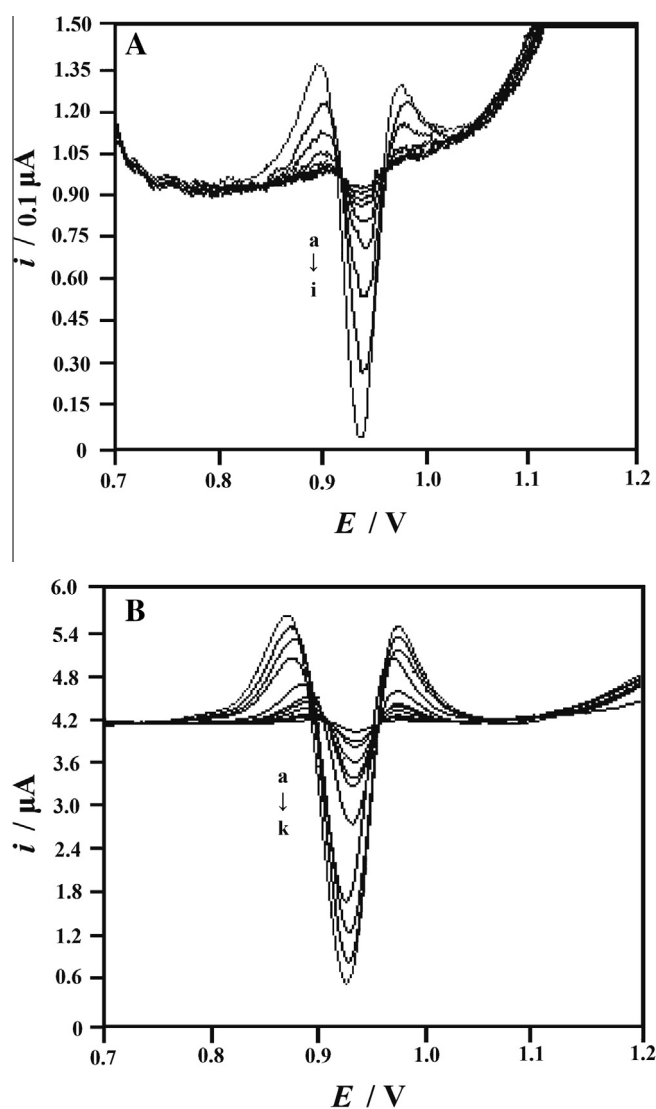


**Fig. 4.** Second-order derivative linear scan voltammograms of solutions containing various concentrations of vanillin in 0.1 M  $\text{H}_3\text{PO}_4$  at the GR-PVP/ABPE. (A) From a to i: 0.02, 0.04, 0.06, 0.08, 0.1, 0.2, 0.4, 0.6, 0.8  $\mu\text{M}$  vanillin. (B) From a to k: 1, 2, 4, 6, 8, 10, 20, 40, 60, 80 and 100  $\mu\text{M}$  vanillin. Accumulation potential: 0.0 V, accumulation time: 60 s, scan rate: 0.1  $\text{V s}^{-1}$ .

**Table 1**

Comparison with other electrochemical methods for the determination of vanillin.

Electrode	Technique	Supporting electrolyte	Linear range ( $\mu\text{M}$ )	Detection limit ( $\mu\text{M}$ )	References
<sup>a</sup> BDD electrode	<sup>e</sup> SWV	0.1 M phosphate buffer, pH 2.5	3.3–98	0.16	Yardim et al. (2013)
<sup>b</sup> AuPd–graphene/GCE	<sup>f</sup> DPV	0.1 M phosphate buffer, pH 7.0	0.1–7 and 10–40	0.02	Shang et al. (2014)
<sup>c</sup> CDA/Au–AgNPs/GCE	Amperometry	0.1 M phosphate buffer, pH 2.0	0.2–50	0.04	Zheng et al. (2010)
Disposable screen-printed electrode	SWV	0.1 M phosphate buffer, pH 7.4	5–400	0.4	Bettazzi et al. (2006)
PVC–graphite composite electrode	Amperometry	0.2 M $\text{H}_2\text{SO}_4$	660–9200	290	Luque et al. (2000)
Graphene/GCE	DPV	$\text{Na}_2\text{HPO}_4$ – $\text{C}_6\text{H}_8\text{O}_7$ buffer, pH 5.0	0.6–48	0.056	Peng et al. (2012)
<sup>d</sup> MWCNTs–TAPcCo/GCE	SWV	0.1 M phosphate buffer, pH 7.2	4.2–5000	0.44	Kong et al. (2010)
GR–PVP/ABPE	Derivative voltammetry	0.1 M $\text{H}_3\text{PO}_4$	0.02–2.0, 2.0–40 and 40–100	0.01	This work

<sup>a</sup> Boron-doped diamond electrode.<sup>b</sup> AuPd nanoparticles–graphene composite modified glassy carbon electrode.<sup>c</sup> Cellulose diacetate/Au–Ag alloy nanoparticles modified glassy carbon electrode.<sup>d</sup> Multi-walled carbon nanotubes chemically modified by 2,9,16,23-tetraaminophthalocyaninatocobalt modified glassy carbon electrode.<sup>e</sup> Square-wave voltammetry.<sup>f</sup> Differential pulse voltammetry.**Table 2**Determination of vanillin in food samples ( $n = 4$ ).

Sample <sup>a</sup>	Found by this method <sup>b</sup> ( $\mu\text{M}$ )	Added ( $\mu\text{M}$ )	Total found by this method <sup>b</sup> ( $\mu\text{M}$ )	Recovery (%)	Content determined by this method <sup>b</sup> ( $\mu\text{g g}^{-1}$ )	Content determined by HPLC <sup>b</sup> ( $\mu\text{g g}^{-1}$ )
Biscuit 1	0.30 ( $\pm 0.01$ )	0.30	0.62 ( $\pm 0.03$ )	106.7	9.3 ( $\pm 0.4$ )	9.4 ( $\pm 0.5$ )
Biscuit 2	1.40 ( $\pm 0.06$ )	1.00	2.43 ( $\pm 0.11$ )	103.0	42.6 ( $\pm 1.8$ )	42.4 ( $\pm 1.8$ )
Chocolate 1	2.45 ( $\pm 0.09$ )	2.00	4.38 ( $\pm 0.17$ )	96.5	74.6 ( $\pm 2.9$ )	74.9 ( $\pm 2.8$ )
Chocolate 2	5.93 ( $\pm 0.22$ )	5.00	10.87 ( $\pm 0.47$ )	98.8	180.5 ( $\pm 6.6$ )	180.4 ( $\pm 6.7$ )
Candy	1.21 ( $\pm 0.04$ )	1.00	2.18 ( $\pm 0.08$ )	97.0	36.7 ( $\pm 1.2$ )	36.9 ( $\pm 1.2$ )
Cake	10.76 ( $\pm 0.34$ )	10.00	20.60 ( $\pm 0.75$ )	98.4	327.4 ( $\pm 10.4$ )	327.4 ( $\pm 10.3$ )
Orange flavored soft drink	ND <sup>c</sup>	0.50	0.52 ( $\pm 0.03$ )	104.0	ND	ND
Colo	ND	2.00	1.97 ( $\pm 0.09$ )	98.5	ND	ND
Icecream	7.76 ( $\pm 0.30$ )	7.00	14.63 ( $\pm 0.58$ )	98.1	236.2 ( $\pm 9.0$ )	236.2 ( $\pm 9.3$ )
Soy milk powder	4.36 ( $\pm 0.15$ )	4.00	8.42 ( $\pm 0.32$ )	101.5	132.9 ( $\pm 4.7$ )	133.0 ( $\pm 4.5$ )

<sup>a</sup> All samples were collected from local supermarkets.<sup>b</sup> Average  $\pm$  confidence interval, the confidence level is 95%.<sup>c</sup> Not detected.

or comparable to the reported electrodes in terms of linear range and detection limit. Additionally, simplicity, low cost, high selectivity and environmental friendly material used in the fabrication of the electrode make it attractive sensor in vanillin analysis.

### 3.8. Practical applications

In order to evaluate the performance of GR–PVP/ABPE by practical analytical applications, the determination of vanillin was carried out in real commercial food samples. The samples were prepared as described in Section 2.5. Each pretreated sample solution was transferred to a voltammetric cell and analyzed in the day of preparation. The second-order linear scan voltammetric measurements were carried out in the potential range from 0.7 V to 1.2 V under the optimal conditions developed for the pure vanillin. The content of vanillin was determined by means of calibration curve method. Table 2 presented the determination results for four parallel measurements. It was found a concentration of 0.30–10.76  $\mu\text{mol L}^{-1}$  of vanillin in the measurement cell. Taking into account the dilution of the sample, it was calculated that the amount of vanillin present in the samples was 9.3–327.4  $\mu\text{g g}^{-1}$ . The recovery experiments were also performed by measuring the voltammetric responses to the samples in which the known concentrations of vanillin standard solution were added. The recoveries were in the range of 96.5–106.7%. For comparison, the samples were also determined with a reference method of high-performance liquid chromatography (HPLC). As shown in Table 2, the results obtained by this proposed method were in good agreement

with those obtained by HPLC method. These results demonstrated that the modified electrode has satisfactory analytical performance and it can be a feasible sensor for determination of vanillin in commercial food samples.

### 4. Conclusions

In this work, we have studied the electrochemical behavior of vanillin at an acetylene black paste electrode modified with graphene–polyvinylpyrrolidone composite film. The results indicate that polyvinylpyrrolidone can be used as an excellent disperser to ensure graphene to be stably and uniformly dispersed in water, and the as-prepared graphene–polyvinylpyrrolidone composite exhibits a high electrochemical activity for promoting the direct electron transfer of vanillin. At the same time, acetylene black was introduced to amplify vanillin signal. In comparison with the poor response at conventional carbon paste electrode, the signal for vanillin at the modified electrode was greatly improved. The preparation conditions for the sensor, suitable operating conditions, calibration curve, detection limit and selectivity in vanillin detection were presented and discussed. Under the optimal conditions, the presented method can provide wider linear range and lower detection limit compared with other previous procedures. Besides, this new method shows a significant improvement in simplifying electrode preparation, saving time and lowering cost. The graphene–polyvinylpyrrolidone nanocomposite developed here may offer a new approach for developing novel types of highly sensitive and stable electrochemical sensors.



## Acknowledgments

This work was supported by the Project of National Natural Science Foundation of China (Nos. 21105024 and 21472038), the Project of Science and Technology Department of Hunan Province (2014SK3178) and the Key Discipline Project of Hunan Province.

## Appendix A. Supplementary data

Supplementary data associated with this article can be found, in the online version, at <http://dx.doi.org/10.1016/j.foodchem.2015.02.035>.

## References

- Anson, F. C. (1964). Application of potentiostatic current integration to the study of the adsorption of cobalt (III)-(ethylenedinitrilo(tetraacetate) on mercury electrodes. *Analytical Chemistry*, 36, 932–934.
- Bard, A. J., & Faulkner, L. R. (2001). *Electrochemical methods: Fundamentals applications* (2nd ed.). New York: Wiley.
- Bettazzi, F., Palchetti, I., Sisalli, S., & Mascini, M. (2006). A disposable electrochemical sensor for vanillin detection. *Analytica Chimica Acta*, 555, 134–138.
- Deng, P., Xu, Z., & Feng, Y. (2014). Acetylene black paste electrode modified with graphene as the voltammetric sensor for selective determination of tryptophan in the presence of high concentrations of tyrosine. *Materials Science and Engineering C*, 35, 54–60.
- Deng, P., Xu, Z., & Kuang, Y. (2013). Electrochemically reduced graphene oxide modified acetylene black paste electrode for the sensitive determination of bisphenol A. *Journal of Electroanalytical Chemistry*, 707, 7–14.
- Farthing, D., Sica, D., Abernathy, C., Fakhry, I., Roberts, J. D., Abraham, D. J., et al. (1999). High-performance liquid chromatographic method for determination of vanillin and vanillic acid in human plasma, red blood cells and urine. *Journal of Chromatography B: Biomedical Sciences and Applications*, 726, 303–307.
- Galus, Z. (1976). *Fundamentals of electrochemical analysis*. Chichester: Ellis Horwood.
- Gan, T., Shi, Z., Deng, Y., Sun, J., & Wang, H. (2014). Morphology-dependent electrochemical sensing properties of manganese dioxide-graphene oxide hybrid for guaiacol and vanillin. *Electrochimica Acta*, 147, 157–166.
- Gooding, J. J., Praig, V. G., & Hall, E. A. H. (1998). Platinum-catalyzed enzyme electrodes immobilized on gold using self-assembled layers. *Analytical Chemistry*, 70, 2396–2402.
- Hardcastle, J. L., Paterson, C. J., & Compton, R. G. (2001). Biphasic sonoelectroanalysis: Simultaneous extraction from, and determination of vanillin in food flavoring. *Electroanalysis*, 13, 899–905.
- Huang, L., Hou, K., Jia, X., Pan, H., & Du, M. (2014). Preparation of novel silver nanoplates/graphene composite and their application in vanillin electrochemical detection. *Materials Science and Engineering C*, 38, 39–45.
- Kong, D. J., Shen, S. F., Yu, H. Y., Wang, J. D., & Chen, N. S. (2010). Chemical modification of multi-walled carbon nanotubes by tetraaminophthalocyaninatocobalt for the electrocatalytic oxidation of vanillin. *Chinese Journal of Inorganic Chemistry*, 26, 817–821.
- Laviron, E. (1974). Adsorption, autoinhibition and autocatalysis in polarography and in linear potential sweep voltammetry. *Journal of Electroanalytical Chemistry and Interfacial Electrochemistry*, 52, 355–393.
- Li, D., & Kaner, R. B. (2008). Graphene-based materials. *Science*, 320, 1170–1171.
- Li, D., Müller, M. B., Gilje, S., Kaner, R. B., & Wallace, G. G. (2008). Processable aqueous dispersions of graphene nanosheets. *Nature Nanotechnology*, 3, 101–105.
- Liu, S. M., Li, J. N., & Mao, X. (2003). Stripping voltammetric determination of zirconium with complexing preconcentration of zirconium(IV) at a morin-modified carbon paste electrode. *Electroanalysis*, 15, 1751–1755.
- Longares-Patrón, A., & Cañizares-Macías, M. P. (2006). Focused microwaves-assisted extraction and simultaneous spectrophotometric determination of vanillin and p-hydroxybenzaldehyde from vanilla fragans. *Talanta*, 69, 882–887.
- Luque, M., Luque-Pérez, E., Ríos, A., & Valcárcel, M. (2000). Supported liquid membranes for the determination of vanillin in food samples with amperometric detection. *Analytica Chimica Acta*, 410, 127–134.
- Meyer, J. C., Geim, A. K., Katsnelson, M. I., Novoselov, K. S., Booth, T. J., & Roth, S. (2007). The structure of suspended graphene sheets. *Nature*, 446, 60–63.
- Niyogi, S., Bekyarova, E., Itkis, M. E., McWilliams, J. L., Hamon, M. A., & Haddon, R. C. (2006). Solution properties of graphite and graphene. *Journal of the American Chemical Society*, 128, 7720–7721.
- Ohashi, M., Omae, H., Hashida, M., Sowa, Y., & Imai, S. (2007). Determination of vanillin and related flavor compounds in cocoa drink by capillary electrophoresis. *Journal of Chromatography A*, 1138, 262–267.
- Pasricha, R., Gupta, S., & Srivastava, A. K. (2009). A facile and novel synthesis of Ag-graphene-based nanocomposites. *Small (Weinheim an der Bergstrasse, Germany)*, 5, 2253–2259.
- Peng, J., Hou, C., & Hu, X. (2012). A graphene-based electrochemical sensor for sensitive detection of vanillin. *International Journal of Electrochemical Science*, 7, 1724–1733.
- Pérez-Silva, A., Odoux, E., Brat, P., Ribeyre, F., Rodriguez-Jimenes, G., Robles-Olvera, V., et al. (2006). GC-MS and GC-olfactometry analysis of aroma compounds in a representative organic aroma extract from cured vanilla (*Vanilla planifolia* G. Jackson) beans. *Food Chemistry*, 99, 728–735.
- Shang, L., Zhao, F., & Zeng, B. (2014). Sensitive voltammetric determination of vanillin with an AuPd nanoparticles-graphene composite modified electrode. *Food Chemistry*, 151, 53–57.
- Teissedre, P. L., & Waterhouse, A. L. (2000). Inhibition of oxidation of human low-density lipoproteins by phenolic substances in different essential oils varieties. *Journal of agricultural and Food Chemistry*, 48, 3801–3805.
- Timotheou-Potamia, M., & Calokerinos, A. C. (2007). Chemiluminometric determination of vanillin in commercial vanillin products. *Talanta*, 71, 208–212.
- Velasco, J. G. (1997). Determination of standard rate constants for electrochemical irreversible processes from linear sweep voltammograms. *Electroanalysis*, 9, 880–882.
- Waliszewski, K. N., Pardio, V. T., & Ovando, S. L. (2006). A simple and rapid HPLC technique for vanillin determination in alcohol extract. *Food Chemistry*, 101, 1059–1062.
- Walton, N. J., Mayer, M. J., & Narbad, A. (2003). Vanillin. *Phytochemistry*, 63, 505–515.
- Yardı, Y., Gülcen, M., & Şentürk, Z. (2013). Determination of vanillin in commercial food product by adsorptive stripping voltammetry using a boron-doped diamond electrode. *Food Chemistry*, 141, 1821–1827.
- Zheng, D., Hu, C., Gan, T., Dang, X., & Hu, S. (2010). Preparation and application of a novel vanillin sensor based on biosynthesis of Au-Ag alloy nanoparticles. *Sensors and Actuators B: Chemical*, 148, 247–252.